ZIBELINE INTERNATIONAL™ PUBLISHING
ISSN: 2590-4043
CODEN: AEMCDV

Acta Electronica Malaysia (AEM)

DOI: http://doi.org/10.26480/aem.01.2023.08.14

RESEARCH ARTICLE

# MODELLING AND COMPARATIVE ANALYSIS OF INDUCTIVELY COUPLED CIRCULAR AND SQUARE LOOP WIRELESS POWER TRANSFER AT UHF BAND FOR AUTOMOBILE CHARGING

**Adeniran, Adebayo Olusakin[a], Olabisi, Olusegun[b], Akankpo[a], Akaninyene Okon[a], Umoren, Emmanuel Bassey[a], Udo, Kufre Israel[a], Oliver Odira Anyanor[c], Agbasi, Ebuka Okechukwu[d*]**

[a]Department of Physics, University of Uyo, Uyo, Akwa Ibom State, Nigeria.
[b]Department of Science Laboratory Technology, Lautech, Ogbomoso, Oyo State, Nigeria.
[c]Department of Physics and Industrial Physics, Nnamdi Azikwe University, Awka, Anambra State, Nigeria.
[d]Geo-Okan Nigeria Limited, Eket, Akwa Ibom State, Nigeria.
*Corresponding Author Email: agbasi.okechukwu@gmail.com



**ARTICLE DETAILS**

*Article History:*

Received 23 May 2023
Revised 27 June 2023
Accepted 01 August 2023
Available online 15 August 2023

**ABSTRACT**

Electric cars are now in high demand in every part of the world in order to minimise fossil fuel usage, which in turn will reduce environmental pollution with a view to achieving a green environment. Wireless Power Transmission (WPT) is now becoming a technology that is highly sought globally. Wireless Power Transmission is an approved and achieving technology, uncovering its applications in various fields. Power is transferred from a source to an electrical load without the need for interconnection. In this research, inductively square and circular loop wireless power transfer was simulated, modelled and analysed for charging cars (Electric Vehicles). The effects of orientation and alignment, as well as coupling losses, of transmitting and receiving loops were observed. Square and circular loop sizes and orientation were determined. Simulation was accomplished using the electromagnetic system COMSOL Multiphysics 5.5 at a frequency domain of 1.8MHz. Results obtained from the simulation showed a strong coupling at 0 degrees and a heat coupling around the receiving antenna at an angle of 90 degrees for the square loop, while the circular loop displayed perfect coupling at all angles, with average electromagnetic wave energy/power flow for both circular and square ranges from 3.4433 to 12.308Wm² and directivity of 6.7502 and 1.3018dB, respectively, which makes the circular loop more acceptable for electrical vehicle charging. The radiating coupling power at different varying angles depends on their reflection coefficient (S-parameters), which explain how much power is reflected and how the variation in the position and orientation of the loops affects the mutual coupling. These results indicate that a square loop is good for direct charging while a circular loop is absolutely perfect for both direct and indirect charging.

**KEYWORDS**

electric vehicle, substrate, wireless, COMSOL, transfer, and noncontact.

## 1. Introduction

The transportation sector remains a major contributor to global climate change and carbon dioxide emissions. With about 60 to 70% of the global oil consumption in transportation in 2017, the need for a clean alternative is eminent and urgent. Electric vehicles are an important pillar of this transition towards a clean energy society. Electric vehicles have recently been significantly developed in terms of both performance and drive range.

The noncontact electricity transmission method for supplying electricity to an electrical apparatus is based on Faraday's law of electromagnetic induction and its recent (less than 20-year old) development in the field of household appliances (Hidetoshi, 2018). Wireless Power Transfer (WPT) is well suited for medical applications. The concept of wireless power transfer has been introduced since the 19th century. In the 1890's, Tesla demonstrated the first near-field coupling system that wirelessly powered a lamp based on a two-coil system (Adeniran et al., 2018; Tesla, 1891). Resonant circuits were used to enhance the transmission range. Years later, the coil was introduced to perform similar experiments (Divyabharathi et al., 2019; Kurs et al., 2007; Lu et al., 2014).

Wireless power transfer technology is based on the principle of energy coupling via antenna orientation (Gautami et al., 2018; Olabisi et al., 2019; Zhang et al., 2016). This technology has the ability to charge multiple electronic devices concurrently, over a long distance and through materials such as glass, plastic, and wood.

The printed loop antenna was recently introduced to wireless power transfer and is now used in electronic gadgets, smart phones, wearable electronics, RFID trackers, the medical industry for medical implants to replace power cords or replaceable batteries in heart pumps, and hybrid electric vehicles (COMSOL). The wireless power transfer (WPT) technology uses an electromagnetic field to transfer energy between two objects. The power source is connected to a power transmitting unit (PTU) which generates a magnetic field and a power receiving unit (PRU) that converts energy into usable power (John, 2020).

A loop is a closed-circuit antenna, that is, one in which a conductor is formed into one or more turns so that its two ends are close together. Loops can be divided into two general classes: those in which both the total conductor length and the maximum linear dimension of a turn are very small compared with the wavelength, and those in which both the

| Quick Response Code | Access this article online | |
|---|---|---|
| | **Website:** www.actaelectronicamalaysia.com | **DOI:** 10.26480/mecj.01.2023.08.14 |

Cite The Article: Adeniran, Adebayo Olusakin, Olabisi, Olusegun, Akankpo, Akaninyene Okon, Umoren, Emmanuel Bassey, Udo, Kufre Israel, Oliver Odira Anyanor, Agbasi, Ebuka Okechukwu (2023). Modelling And Comparative Analysis of Inductively Coupled Circular and Square Loop Wireless Power Transfer at Uhf Band for Automobile Charging. *Acta Electronica Malaysia, 7(1): 08-14.*

conductor length and the loop dimensions begin to be comparable with the wavelength [9]. A "small" loop can be considered to be simply a rather large coil, and the current distribution in such a loop is the same as in a coil. That is, the current has the same phase and the same amplitude in every part of the loop. To meet this condition, the total length of the conductor in the loop must not exceed about 0.1. A "large" loop is one in which the current is not the same either in amplitude or phase in every part of the loop. This change in current distribution gives rise to entirely different properties as compared with a small loop.

### 1.1 Basic Theory of Wireless Power Transfer (WPT)

When electrical energy from an alternating current (AC) power supply such as a commercial power supply or from a direct current (DC) power supply such as solar cells is converted to high frequency electrical energy by using a high frequency inverter, a wireless feeding device (TX) releases electrical energy through a transmission device into space. Then the receiving system (Rx) converts the electrical power into DC in the recipient electrical appliance, as shown in Figure 1a and 1b. A key feature of non-contact electricity transmission is the distribution of electromagnetic energy over space by using an electromagnetic field wave.

The wireless power transfer model analyses the energy coupling between two circular loop antennae. The model describes the wireless power transfer technology by evaluating the shape of the loop antennae energy coupling tuned for the UHF RFID frequency. The antenna is designed by reducing its size using chip inductors. S-parameters are investigated for proper coupling by configuring the transmitting antenna as a fixed type while the receiving antenna is a rotating type. The model is designed as a perfect electric conductor (PEC). The antennas are made of a material called polytetrafluoroethylene (PTFE) board and have a thin copper layer on top. Each of the antennae is featured as a lumped inductor and a lumped port that can resonate or terminate the loop antenna (Bhuvaneswari and Latha, 2015).

The antennas are perfectly shaped to perform inductive coupling. Considering ampere circuital law, loop integral of the $\vec{B}$ field equals the net current I enclosed in a loop.

$$\Phi \vec{B}.\vec{dl} = \mu i \tag{1}$$

Where $\vec{B}$ = magnetic flux density, I = net current and $\mu$ = permeability

According to Biot-Savart Law,

$$dB = \frac{\mu \times i \times dl \times \sin\theta}{4\pi r^2} \tag{2}$$

dl is infinitesimal length of the conducting material carrying electric charge (i), r is distance from the length element dl to the field point P.

Magnetic flux is expressed by equation below:

$$\phi_s = \iiint \hat{o}\, \vec{B} d \vec{A} \tag{3}$$

Where A is the area enclosed in the given loop.

Solving the differential

$$\phi_s \phi \frac{dl}{\mu A \times \ell} \equiv i \tag{4}$$

Amperes law in term of reluctance is given by:

$$\phi_s = \frac{i}{R_m} \tag{5}$$

Where, $R_m$ is the reluctance of the magnetic loop and it is represented in the equation given as;

$$\left[\frac{A}{W_b}\right]\left[R_m = \phi \frac{dl}{\mu A \times l}\right] \tag{6}$$

Considering the Faradays law,

$$\oint E.dl = \frac{d\phi_B}{dt} \tag{7}$$

$\vec{E}$ is the electromotive force (emf), $\phi_B$ is the magnetic flux.

The coil voltage is given by;

$$v_1(t) = L_p \frac{di_1(t)}{dt} + M \frac{di_2(t)}{dt} \tag{8}$$

$$v_2(t) = L_s \frac{di_2(t)}{dt} + M \frac{di(t)}{dt} \tag{9}$$

Where $V_1$(t) and $V_2$ (t) are voltage in the primary winding and secondary winding respectively, $L_P$ and $L_S$ are primary and secondary self inductance respectively and M is the mutual inductance. Coupling coefficient k along with the inductance ratio n is given by:

$$k = \frac{M}{\sqrt{L_p L_s}} \tag{10}$$

$$n = \sqrt{\frac{L_s}{L_p}} \tag{11}$$

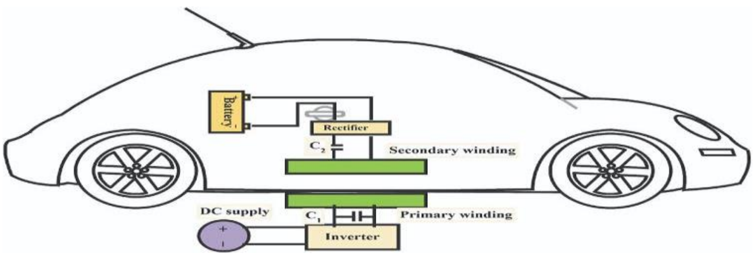


(a)

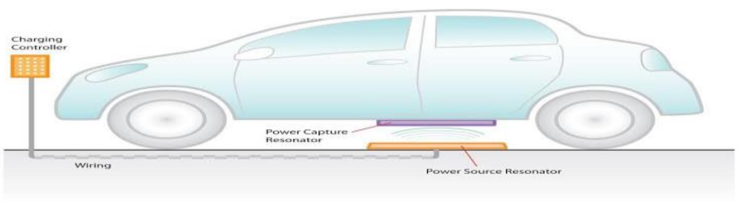


(b)

**Figure 1:** Automobile (Electric Vehicle) using Wireless Power Transfer

## 2. Loop Coil Design

The antenna operates under the fundamental mode with frequency of operation ($f_1$), dielectric constant of substrate ($\epsilon_r$), the substrate height (h), length of the proposed printed loop, width of the loop required**.** The dielectric constant of the substrate material plays an important role in the

Cite The Article: Adeniran, Adebayo Olusakin, Olabisi, Olusegun, Akankpo, Akaninyene Okon, Umoren, Emmanuel Bassey, Udo, Kufre Israel, Oliver Odira Anyanor, Agbasi, Ebuka Okechukwu (2023). Modelling And Comparative Analysis of Inductively Coupled Circular and Square Loop Wireless Power Transfer at Uhf Band for Automobile Charging. *Acta Electronica Malaysia, 7(1): 08-14.*

printed antenna design. A substrate with a high dielectric constant reduces the dimensions of the patch, which also affects the antenna performance. There is always a relationship between the patch size and the performance of the system. Here are the design procedures for the circular and square loops.

### 2.1 Circular Loop Design

The inductive coupling method of a circular loop shown in Figure: 2(II) is based on electromagnetic induction and was developed by Michael Faraday in 1831 (Misrad et al., 2020). The lumped inductor inserted in this design was to reduce the size of the loop and to distribute the energy equally round the loop. To ensure uniform current distribution in the loop, loop radius, $a$ must satisfy the condition given by;

$$\boldsymbol{a} < 0.016\boldsymbol{\lambda} \tag{12}$$

Where $\lambda$ is equal to wavelength; the frequency band chosen is 1.85MHz. The centre frequency $f_C$ is obtained from $f_C$ given as:

$$f_c = \frac{v}{\lambda} \tag{13}$$

The wavelength $\boldsymbol{\lambda}$ is given as:

$$\lambda = \frac{v}{f_c} \tag{14}$$

From equation 15, the radius of the loop must be less than 5.08mm. Therefore, the design model was obtained using the following guidelines Objective Function: Maximum (radiation resistance) and Minimum (Ohm resistance) Subject to the radiation resistance $R_r$ for $n$ turns of wire is given by Lu et al. 2014.

$$R_r = \frac{20\pi^2 C^4}{\lambda^4} \tag{15}$$

$$C = 2\pi a$$

Radiation resistance for a single turn is given as:

$$R_r = \eta \frac{8}{3}\pi^3 \left( N \frac{A}{\lambda^2} \right)^2 \tag{16}$$

The loss resistance of a loop with N turns, wire radius b, and loop separation 2c. Ohmic resistance per unit length due to proximity effect might be larger than that due to the skin effect. The loos resistance is calculated by:

$$R_l = \frac{N_a}{b} R_s \left( \frac{R_p}{R_0} + 1 \right) \tag{17}$$

### 2.2 Square Loop Design

For the square loop, the effective dielectric constant of the substrate ($\epsilon_{reff}$) is related to the substrate height (h), length of the proposed printed loop and the width of the loop required as given by;

$$\epsilon_{reff} = \frac{\epsilon_r + 1}{2} + \frac{\epsilon_r - 1}{2}\left[1 + 12\frac{h}{W}\right]^{-\frac{1}{2}} \tag{18}$$

Where $\epsilon_r$ is the dielectric constant of the substrate, the length of the printed loop is given as;

$$\Delta L = 0.142h \frac{(\epsilon_{reff} + 0.3)\left(\frac{W}{h} + 0.264\right)}{(\epsilon_{reff} - 0.258)\left(\frac{W}{h} + 0.8\right)} \tag{19}$$

The actual length L, of the patch is given by

$$L = \frac{1}{2f\sqrt{\epsilon_{eff}\sqrt{\mu_0 \epsilon_0}}} - 2\Delta L \tag{20}$$

Where $f$ is frequency, $\mu_0$ is permeability of free space and $\epsilon_0$ is the permittivity of free space of dielectric constant of vacuum. Effective length is given as:

$$L_{eff} = L + 2\Delta L \tag{21}$$

The width (W) of the required loop is given as;

$$W = \frac{1}{2f_r\sqrt{\mu_0\epsilon_0}}\sqrt{\frac{2}{(\epsilon_r + 1)}} \tag{22}$$

Where $f_r$ is resonance frequency. For square printed loop the perimeters are equal as shown in Figure 2 (I).

$$L = W \tag{23}$$

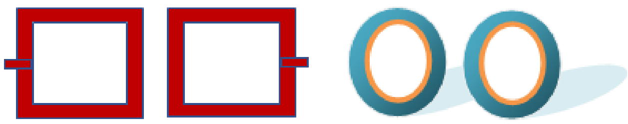


**Figure 2:** Proposed Square loop and Circular loop

The loop inductance is determined by using the equation:

$$L_{Square} = \frac{2n^2\mu a}{n}\left(ln\frac{a}{d} - 0.774\right) \tag{24}$$

Where

*n-Number of coils,*

*d - wire diameter,*

*a - length of the patch and*

*L – Inductance while the inductor used for this work is obtained to be 0.006514nH*

Magnetic field and electric field are inductively generated in the space near a frequency power supply (e.g. KHz – MHz range). Receivers received power wirelessly through magnetic and electric fields; this is called inductive coupling WPT as shown in Figure 3 (Van and Puers, 2009).

The power received in the radiative near field is given in Equation 25, when r is sufficiently small.

$$P_t = \left(1 - e^{-r^2}\right)P \tag{25}$$

$$r^2 = \frac{A_t A_r}{(\lambda d)^2} \tag{26}$$

The mutual inductance between the transmitter and receiver is obtained using Equation 27:

$$M = k \times \sqrt{(L_1 \times L_2)} \tag{27}$$

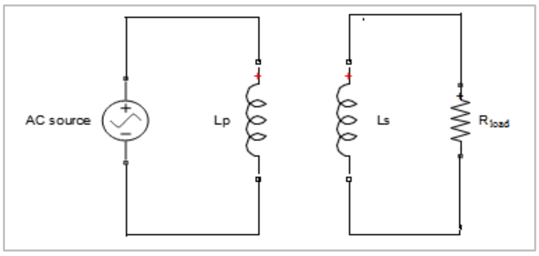


**Figure 3:** Basic circuit diagram of WPT using inductive coupling (Van & Puers, 2009)

## 3. COMSOL MULTIPHYSICS 5.5.

COMSOL Multiphysics is a cross-platform finite element analysis solver and multiphysics simulation software. It allows conventional physics-based user interfaces and coupled systems of partial differential equations (PDE). COMSOL provides an IDE and a unified workflow for electrical, mechanical, fluid, acoustic, and chemical applications.

### 3.1 Model Definition and Simulation

The modelling and simulation were conducted using COMSOL Multiphysics 5.5, which is a general-purpose modelling software and perfect software for electromagnetic systems simulation. The model consists of two printed square loop antennas enclosed by an air domain with a perfectly matched layer (PML). The etched layer is patterned on a 2 mm Polytetrafluoroethylene (PTFE) board. The thickness of the copper layer is geometrically much thicker than the copper skin depth, so it is modelled as a perfect electric conductor (PEC). These processes follow the procedures for modelling a perfectly conducting system in the electromagnetic wave and frequency domains along with the frequency domain for physics study, and the frequency was set to 1.8MHz. Geometry for the loop was drawn using the work plane where the square point was taken and drew at the centre of the graphics plane following the perimeter obtained for the loop antenna. These processes were followed for the inner patch (Brown, 1984; Ding, 2015). The receiving loop was mirrored to form an antenna of the same structure and size, which was placed inside a perfectly conducting sphere to form a layer around the modelled systems.

The required modelling equations are as follows:

Frequency domain equation for the simulation is as follows:

$$\nabla X \, \mu_r^{-1}(\nabla XE) - k_0^2\left(\varepsilon_r - \frac{j\sigma}{w\varepsilon_0}\right) \in = 0 \qquad (28)$$

Where $\mu_r$ is permeability of the substrate $j$ is the charge density, σ is the conductivity, ω is the frequency domain and E is the electric field intensity.

and Perfect Electric is given as;

$$n \, X \, E = 0 \qquad (29)$$

While lumped port is represented by equation 27;

$$Z = \frac{V_1}{j_1} \qquad (30)$$

Resonant frequency = 1.8MHz.

Now that the modelling equations have been clearly stated, it is also important to tabulate the necessary simulation parameters as shown in Table 1 for circular loop and Table 2 for square loop. The 3-dimensional (3-D) analysis of a square loop meshed system shown in Figure 4 and its corresponding 3-D analysis when placed in a perfect conducting region shown in Figure 5.

**Table 1:** Circular loop Simulation Parameters

| Loop | Length (cm) | Width (cm) | Position (xy, xy) cm |
|---|---|---|---|
| Circular ring 1 | 3.6 | 3.6 | 0, 0 |
| Circular ring 2(inner ring) | 3.3 | 3.3 | 0, 0 |
| Inductor | 0.2 | 0.125 | 0, -2.1875 |
| Feed Point | 0.2 | 0.125 | 0, 1.724 |
| Feed line 1 | 0.2 | 0.6 | 0.1, -2.25 |
| Feed line 2 | 0.2 | 0.6 | -0.1, -4 |

**Table 2:** Square Loop Simulation Parameters

| Loop | Length (cm) | Width (cm) | Position (xy, xy) cm |
|---|---|---|---|
| Square ring 1 | 3.6 | 3.6 | 0, 0 |
| Square ring 2(inner ring) | 3.3 | 3.3 | 0, 0 |
| Inductor | 0.2 | 0.125 | 0, -2.1875 |
| Feed Point | 0.2 | 0.125 | 0, 1.724 |
| Feed line 1 | 0.2 | 0.6 | 0.1, -2.25 |
| Feed line 2 | 0.2 | 0.6 | -0.1, -4 |

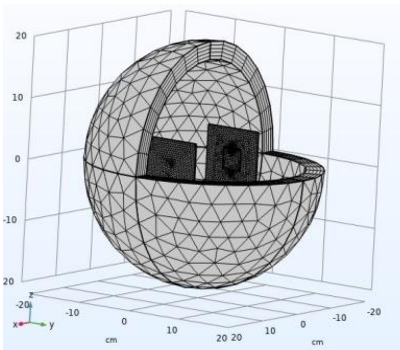

**Figure 4:** Square Loop Meshed System

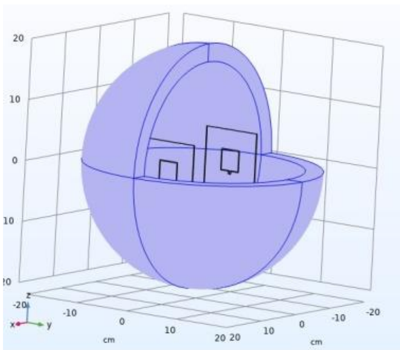

**Figure 5:** Square loop perfectly conducting region

Cite The Article: Adeniran, Adebayo Olusakin, Olabisi, Olusegun, Akankpo, Akaninyene Okon, Umoren, Emmanuel Bassey, Udo, Kufre Israel, Oliver Odira Anyanor, Agbasi, Ebuka Okechukwu (2023). Modelling And Comparative Analysis of Inductively Coupled Circular and Square Loop Wireless Power Transfer at Uhf Band for Automobile Charging. *Acta Electronica Malaysia, 7(1): 08-14.*

## 4. Results and Discussion

The Electric field normalization of the wireless power transfer printed square-loop and circular loop coil were simulated on COMSOL Multiphysics 5.5 software tool where the S-parameters were obtained to determine the coupling capacity of the system, Figure 3 shows the meshed system for applying the physics controlled principle for the calculations, Figure 4, shows the perfectly conducting region of the chip loop, Figure 6a to 6e display the radiating coupling power at different varying angles where their reflection coefficient (S-parameters) which explain the how much power is reflected shows the power presented in Table 3b and 4b, $S_{11}$ is below -20dB regardless of the receiving antenna orientations, while the mutual coupling $S_{21}$ is tabulated with angles for both square and circular loop respectively show the variation in the position and orientation of the loops which not only affect the mutual coupling. Figure 7, shows the S parameters graph against the angles in degrees while Figure 8 and 9 are smith chart and surface admittance graph respectively as shown in Table 3. The smith evaluations display the frequency abilities, perfect impedance matching and admittance for proper applications in the considered field (Ogherohwo et al., 2012).

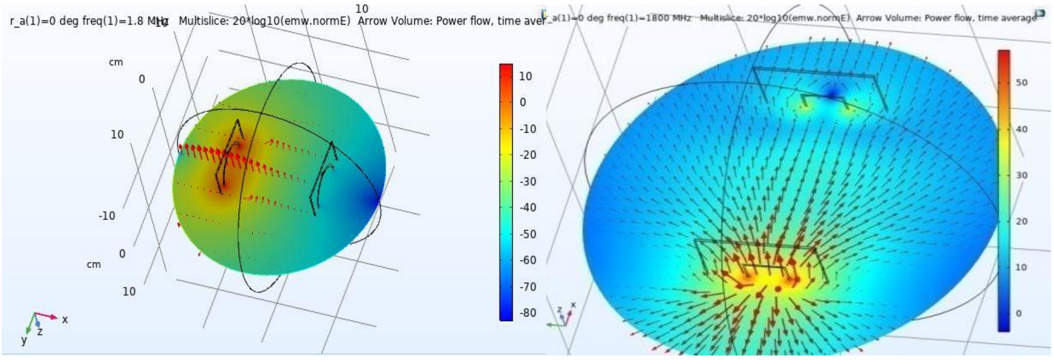


**Figure 6a:** Circular and Square loop Multislice Power flow at 0 degrees

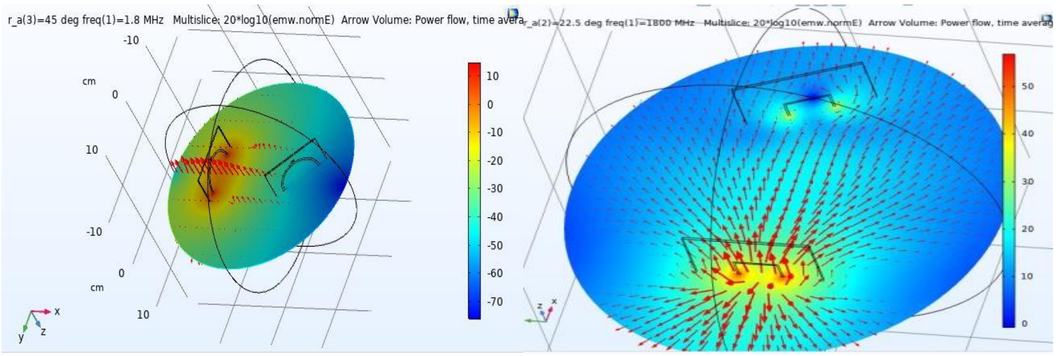


**Figure 6b:** Circular and Square loop Multislice Power flow at 22.5 degrees

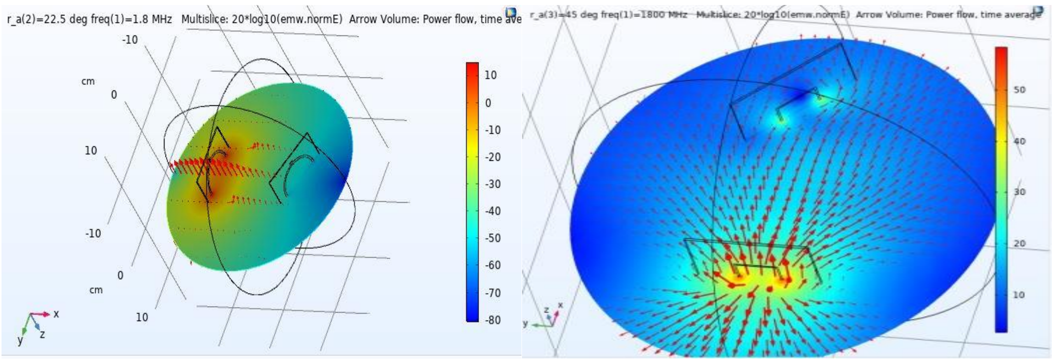


**Figure 6c:** Circular and Square loop Multislice Power flow at 45 degree

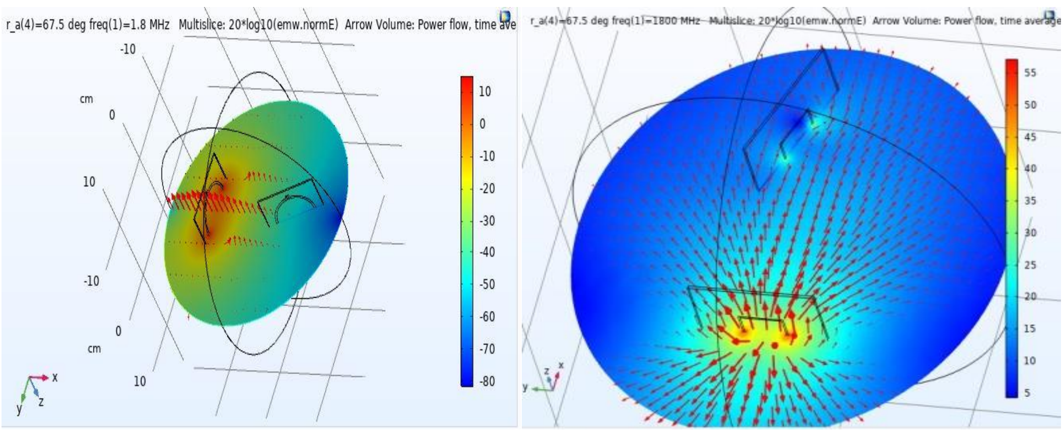


**Figure 6d:** Circular and Square loop Multislice Power flow at 67 degree

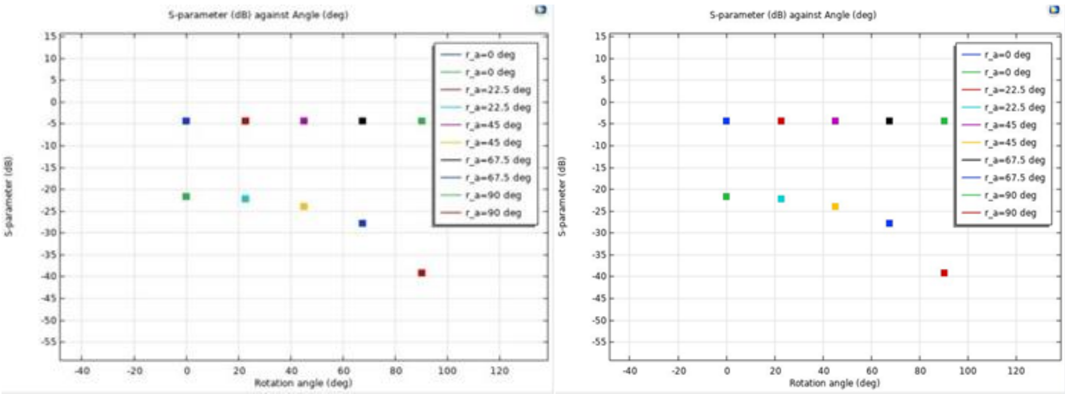


**Figure 7:** Circular and square loop S parameter graph for S11 and S21

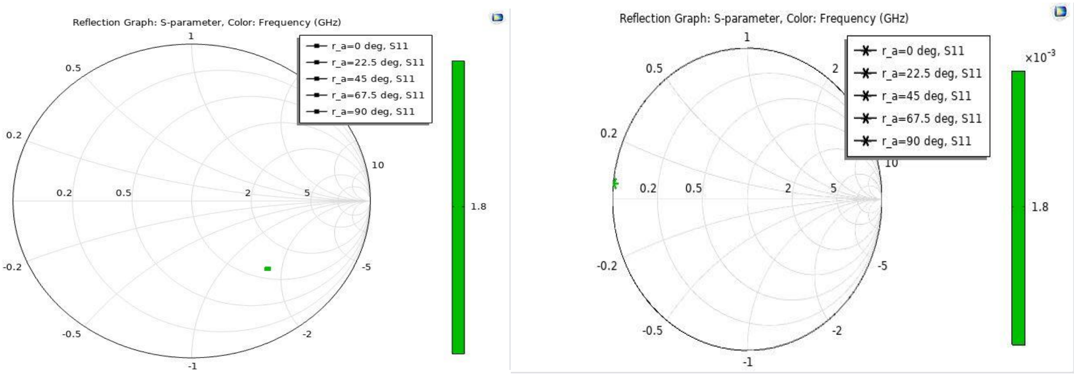


**Figure 8:** Smith Chart for Circular and Square loop

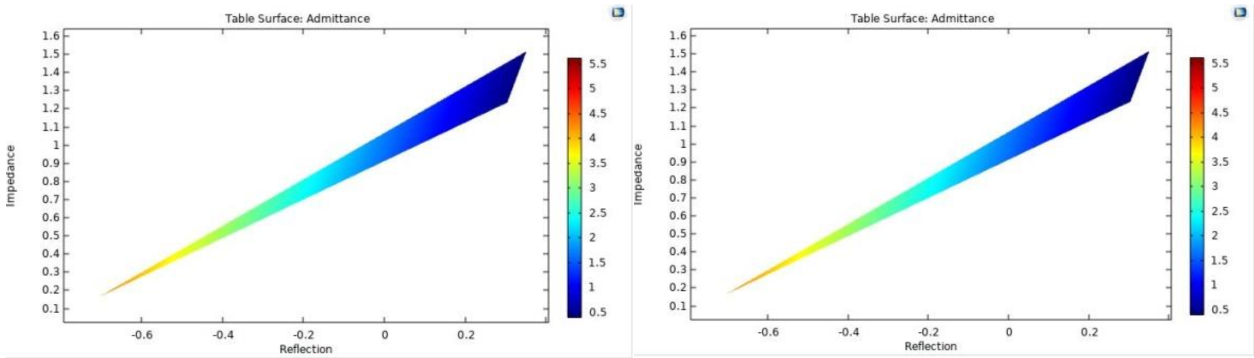


**Figure 9:** Surface Admittance for Circular and Square loops

**Table 3a:** Square loop coil S-Parameters as function of angles

| ANGLE (DEGREE) | 0 | 22.5 | 45 | 67.5 | 90 |
|---|---|---|---|---|---|
| $S_{21}$(dB) | -21.0 | -22.9 | -24.7 | -26.3 | -39.50 |

**Table 3b:** Square loop Coil Smith Evaluation

| Reflection | Impedance | Admittance |
|---|---|---|
| 0.30455 – 0.37273$i$ | 1.2341 – 1.1974$i$ | 0.41740 + 0.40497$i$ |

**Table 4a**: Circular Loop Coil S-Parameters as Function of Angles

| ANGLE (DEGREE) | 0 | 22.5 | 45 | 67.5 | 90 |
|---|---|---|---|---|---|
| $S_{21}$(dB) | -21.9 | -22.0 | -24.0 | -26.0 | -39.01 |

**Table 4b:** Circular loop Coil Smith Evaluation

| Reflection | Impedance | Admittance |
|---|---|---|
| 0.303255 – 0.36373$i$ | 1.1741 – 1.1574$i$ | 0.41740 + 0.40497$i$ |

The power flow time average along the axis was obtained using COMSOL5.5 equations from the energy, power from the electromagnetic wave domain to obtain Tables 5a and 5b:

$$20\, log_{10}(\,emw.normE)$$

Where emw

**Table 5a:** Square Power (W/m²)

| emw.Poav x (W/m²) | emw.Poav y (W/m²) | emw.Poav z (W/m²) |
|---|---|---|
| -28.911 | -1.5599 | 3.4433 |

Cite The Article: Adeniran, Adebayo Olusakin, Olabisi, Olusegun, Akankpo, Akaninyene Okon, Umoren, Emmanuel Bassey, Udo, Kufre Israel, Oliver Odira Anyanor, Agbasi, Ebuka Okechukwu (2023). Modelling And Comparative Analysis of Inductively Coupled Circular and Square Loop Wireless Power Transfer at Uhf Band for Automobile Charging. *Acta Electronica Malaysia, 7(1): 08-14.*

| **Table 5b:** Circular Power in (W/m²) | | |
|---|---|---|
| emw.Poav x (W/m²) | emw.Poav y (W/m²) | emw.Poav z (W/m²) |
| 12.308 | 18.924 | -125.298 |

## 5. Conclusion

The simulation focused on power transfer by analysing the energy and power coupling between two printed square-loop and circular printed antennae carried on the COMSOL Multiphysics 5.5. The antenna design was accelerated in the software using the geometry and other details based on the theory of electromagnetic principles. Five different angles were considered to determine the reception power and identify the coupling energy at exact ranges, as shown in Table 3a for a square loop coil and Table 4a for a circular loop coil. Printed WPT Square-loop and circular antennae chips designed to radiate at a UHF frequency (1.8MHz) provide inherent inductive coupling by their shapes. The perfect coupling configuration was examined in terms of S-parameters by varying the angle of rotation (degrees). A fixed state energy coupling transmitting loop coil was improved, and a receiving printed antenna chip fixed the rotating state.

The square-loop antenna performed excellently well at $0^0$, $22.5^0$ and $67.5^0$ degrees as shown in Figure 6a, 6b and 6c and comparing the admittance, reflection and impedance values for square loop as shown in Tables 3a and 3b has imperfection in coupling and heat coupling at $45^0$ and $90^0$ as observed in Figure. 6d and 6e while the circular has a more excellent performance at every angle compare to square loop as shown in Fig. 4a to 4e for circular loop, the electromagnetic wave from the loops displayed a perfect energy power flow for square along z-axis and circular at both the x and y axes with negative value along other axes shown in Table 5a and 5b above. Therefore, the circular loop would perform absolute well for every angle charging with contact distance wider, but the square loop would require closer distance to avoid the heat coupling during charging. Directivity for the square and circular loops WPT ranges from 1.9768E-14 to 6.7502E-dB. The square-loop and circular loop chips could be applied in automobile charging (EV) through the UHF frequency system.

## References


Adeniran, A.O., Olabisi, O., and Ajao, S.O. 2018. Circuit Simulation and Etching of Distributed Phase Shifter MMIC using Lumped Element Coupler. 2nd World Conference on Applied Science and Technology. (WOCAST 2018). OCT.2018.

Bhuvaneswari, E, and Latha, S. 2015. Bandwidth Enhancement of Proximity-Fed Square-Ring Microstrip Antenna with Different Configurations. International Journal of Advanced Research Trends in Engineering and Technology (IJARTET), 2(5).

Brown, W.C., 1984. The History of Power Transmission by Radio Waves. IEEE Trans Microwave Theory Tech. Vol.32, No 9, 1230-1240.

COMSOL Multiphysics Software.

Ding, Z., 2015. Application of Smart Antenna Technologies in Simultaneous Wireless Information and Power Transfer by exploiting Multi-Antenna Techniques. IEEE Community Magazine53(4):86-93.

Divyabharathi, P., Abirami, M, Puvaneshwari, S., and Vikram, N. 2019. Ring Structured Patch Antenna for Wideband Applications. International Journal of Innovative Technology and Exploring Engineering (IJITEE), 8(5S), 2019.

Gautami, A., Priya, S., Mythili, S., and Baskar, S., 2018. Design and Implementation of Corrugated Circular Loop Antennas in Wireless Power Transfer Technology. Engineering Technology, IIOAB Journal. 9(1),26-29.

Hidetoshi, M. 2018. Basic Theory of Inductive Coupling. Wireless Power Transfer Theory Technology and Applications, the Institution of Engineering and Technology, 2018.

John, J.B., 2020. Loop Antennas for Use On/Off Ground Planes. SAND 2020-4471J.

Kurs, A.A., Karalis, R, Moffatt, J.D., Joannpoulos, P, P, P, Fisher, and Soljacic, M. 2007. Wireless Power Transfer via Strongly Coupled Magnetic Resonance. Science, Vol.317, 83-86.

Lu, X, Wang, P, Niyato, D., Hossan, E. 2014. Dynamic Spectrum Access in Cognitive Radio Networks with RF Energy Harvesting. IEEE Wireless Commun.21 (3):102-110.

Misrad, H.S. and Nasser, H.A. 2020. Wireless Power Transfer via Inductive Coupling: 3C Tecnologia, Glosas de Innovacion aplicadas a la pyme: Edicion Especial Special Issue Abril, 2020.

Ogherohwo, E.P., and Adeniran, A.O., 2012. Design and Performance Analysis of Log Periodic Dipole Antennae at UHF Band. Journal of Electronics and Communication Engineering. IOSR Pg 01 – 04, Vol.13, Issue 3, Sept./Oct.2012.

Olabisi, O, Adeniran, A.O., Ajao, O.S and Areo, S.O. 2019. Design and Performance of Printed Square Log Periodic Array Microstrip Patch Antenna at ".5GHz and 3.5GHz" Journal of Advancement in Communication System (HBRP Publication) 2(3), 2019.

Tesla, N, 1891. Experiments with Alternate Currents of very High Frequency and Their applications to Methods of artificial Illumination. Lecture, America Institute of Electrical Engineers, Colombia College NY, May,1891.

Van Schuylenbergh, K. and Puers, R. 2009. Inductive powering: basic theory and application to biomedical systems. Springer Netherlands. https//www.springer.com/gp/book/9789048124114.

Zhang, J, Yuen, C, Wen, C. K, Jin, S, Wong, K. K, and Zhu, H. 2016. Large System Secrecy Rate Analysis for SWIPT MIMO Wiretap Channels. IEEE Trans. Inf. Forensics Security.11 (1):74-85.